

Simulation and Validation of a GPS Antenna Array Concept for JPALS Application

Ung Suok Kim, Dennis Akos, Per Enge, *Stanford University*
Frederic Bastide, *ENAC, France*

BIOGRAPHY

Ung Suok Kim is a Ph.D. candidate in the Department of Aeronautics and Astronautics at Stanford University. He received B.S.E.s in Aerospace Engineering and Mechanical Engineering from the University of Michigan at Ann Arbor in 1998. He received his M.S. in Aeronautics and Astronautics from Stanford in 2000. His research interest is in GPS antenna arrays, and CRPA algorithms.

Dennis M. Akos completed the Ph.D. degree in Electrical Engineering at Ohio University conducting his graduate research within the Avionics Engineering Center. After completing his graduation he has served as a faculty member with Luleå Technical University, Sweden and is currently a research associate with the GPS Laboratory at Stanford University. His research interests include GPS/CDMA receiver architectures, RF design, and software radios.

Dr. Per Enge is a Professor in the Department of Aeronautics and Astronautics at Stanford University. He received his B.S. in Electrical Engineering from the University of Massachusetts at Amherst in 1975, and his M.S. and Ph.D., both in Electrical Engineering, from the University of Illinois at Urbana-Champaign in 1979 and 1983. Professor Enge's research focuses on the design of navigation systems which satisfy stringent requirements with respect to accuracy, integrity (truthfulness), time availability, and continuity.

Frederic Bastide graduated as an electronics engineer at the ENAC, the French university of civil aviation, in 2001, Toulouse. He is now a Ph.D student at the ENAC. His research focuses on the study of dual frequencies receivers for civil aviation use. Currently he is working on DME/TACAN signals impact on GNSS receivers. He also spent 6 months at the Stanford GPS Lab earlier this year as an exchange researcher.

ABSTRACT

The goal of Joint Precision Approach and Landing System (JPALS) is to provide navigation to support

automatic shipboard landings in zero visibility conditions. The accuracy, integrity and availability requirements for this system are extremely stringent. In order to meet such demanding navigation performance, a dual-frequency carrier phase differential GPS solution is being pursued. In addition, both the shipboard reference station and the airborne user may be subject to multiple hostile jamming sources. The system must be able to continuously provide service with little or no drop in integrity and availability. In order to achieve such stringent performance goals in the difficult operating environment of JPALS, advanced technology will likely be required. One likely element will be the use of an antenna array with digital beam/null steering capabilities to help mitigate jamming and multipath errors.

This paper will present an initial feasibility study for the use of controlled reception pattern antennas (CRPAs) in the JPALS environment. It will present the benefits and the potential difficulties in the implementation of CRPA algorithms for JPALS use. Due to the motion of the ship and the flexure in the antenna mast arm, there may be some uncertainty in the knowledge of the orientation of the shipboard reference antenna array. This uncertainty leads to errors in the carrier phase output of the CRPA.

A simple beam-forming algorithm is presented, and its potential effectiveness for use in JPALS will be presented. The paper concludes by outlining the deficiency associated with the classical beam-forming algorithm implementation for JPALS.

INTRODUCTION

Joint Precision Approach and Landing System (JPALS) is a navigation system being developed to support automatic shipboard landings in zero visibility conditions. The system has extremely stringent accuracy, integrity and availability requirements. Currently, the vertical accuracy is envisioned to be 0.2 meters, with a vertical alarm limit (VAL) of 1.1 meters. The integrity requirement is that the probability of hazardous misleading information must be 10^{-7} , and the system must be available 99.9% of the time under normal conditions [1]. A dual-frequency carrier phase differential GPS solution is being pursued to

meet these navigation performance specifications. On top of these demanding performance requirements, JPALS offers another challenging aspect: its operational environment. The island superstructure and the antenna mast arm on which the reference antenna will be mounted can form a very detrimental multi-path environment. Figure 1 shows a couple of aircraft carrier superstructures that illustrate the potentially nightmarish multi-path environment at the reference antenna location. In addition, both the shipboard reference station and the airborne user may be subject to multiple hostile jamming sources. The system must be able to continuously provide service with greater than 95% availability even with hostile jamming present [1]. Advanced technologies will in all likelihood be required in order to provide service and meet the demanding performance specs. One such technology to be considered will be the use of an antenna array with digital beam/null steering capabilities to help mitigate jamming and reduce multi-path errors.



Figure 1. Examples of superstructures where GPS antenna would be mounted
Left : USS America (CVA-66) Right : USS Enterprise (CVN-65)

However, using a controlled reception pattern antenna (CRPA) for JPALS application does present a difficulty. JPALS, being a carrier phase differential GPS system, requires accurate tracking of the carrier phase at both the reference station and the airborne user to obtain an accurate position fix. The digital beam/null steering is achieved by adjusting each antenna element's output in gain and phase, and combining them to form the array output. If there is any uncertainty in the direction of the beam, the combined CRPA output will not be exactly in phase. With the aircraft carrier pitching and rolling, not to mention the antenna mast arm flexing, there is bound to be uncertainties in the knowledge of the orientation of the antenna array, which leads to uncertainty in the beam-pointing direction. Another potential source of such error is ephemeris error, although such errors are expected to be

detected and accounted for using the integrity monitor algorithms in place.

Immediately, one can see the inherent difficulty in using such an array for JPALS. The output signal from an array may have a carrier phase content that is altered by the adjustments in each element output. The exact nature of this alteration, or change in the phase center of the antenna will have to be known accurately to be of benefit in JPALS, and this is the inspiration behind this research. This paper will present a study of the effects of a beam-forming algorithm on the tracking of the carrier phase signal.

The classic beam-forming algorithm will be presented, along with its potential effectiveness for use in JPALS. A complete software simulation will be presented for a 4 element array in a nominal state (no radio frequency interference (RFI)), and this will be validated with an actual data collection. Also, the ability of the antenna array to acquire signals when it is exposed to RFI will be investigated. Results for CW and pulsed interference injection will be presented. The performance of the carrier tracking loop resulting from a composite antenna array signal is examined as well.

ANALYSIS METHODOLOGY

The beam-forming algorithms and its benefits and effects will be investigated primarily in simulation. In addition, there will be a validation of the software data generation and the beam-forming algorithm implementation using hardware data acquisition of real GPS signals. Figure 2 below shows the flow diagram of the data analysis methods. Four channels of raw intermediate frequency (IF) GPS data will be obtained, either by using the software GPS signal simulator or the hardware data collection system. These data signals are post-processed by the beam-forming module which is implemented in software to produce a one channel beam-formed array output signal. Finally, this output signal is then input to the software receiver to investigate the beam-forming algorithms effects on the performance of signal acquisition and carrier tracking.

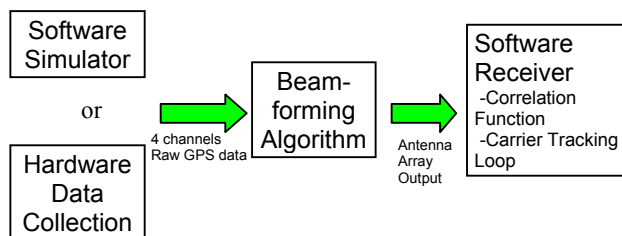


Figure 2. Data Analysis Flow Chart

Software GPS and Interference Signal Simulator

Working with simulated data files affords great flexibility in the cases that can be studied. A GPS signal generator was created in the Labview© environment that generates a simulated single PRN GPS signal at IF. The simulator has an extremely flexible architecture allowing control over numerous parameters such as signal power, sampling frequency, front-end filter bandwidth, filter length, carrier Doppler frequency, C/A code chip delay, etc. One important parameter that can be specified is the phase of the underlying carrier signal generated. This allows for creation of phased signals for each antenna element in the array, according to the incoming LOS direction of the signal. Of course, there is the underlying assumption that the spacing between antenna elements is less than a full wavelength. Currently, the GPS signal generator does not generate navigation messages. It only generates C/A code modulated carrier signals, with the data bits alternating between +1 and -1.

The interference signal generator works through a similar interface, allowing control over parameters such as signal power (J/S), frequency offset from L1, etc. It is also possible to phase these interference signals, allowing for interference signal generation for each antenna element according to the location of the interference source. Currently, four different types of interference signals can be simulated: CW, FM, pulsed, and L1 C/A interference. The software simulator, however, does not currently incorporate any satellite dynamics

Hardware Data Collection System

Real GPS signal data will be used to validate the beam-forming algorithm implementation and the software GPS signal simulator. Figure 3 shows the data collection system. An inexpensive GPS antenna array was constructed using off-the-shelf components. It is a 4 element, 2x2 rectangular configuration array with half-wavelength spacing between antenna elements. Each antenna is a Micropulse Mini-Arinc 26dB active antenna.

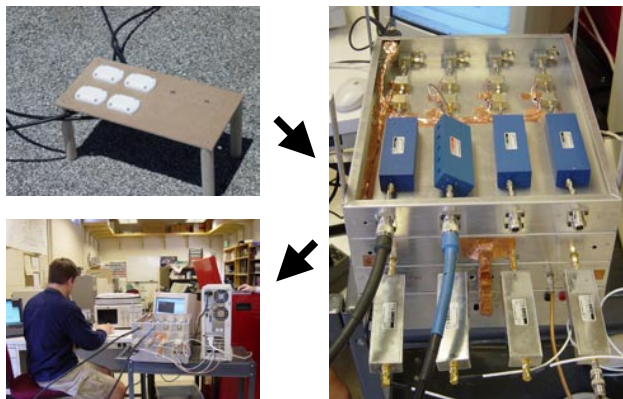


Figure 3. Hardware Data Collection System

The antenna array was placed on top of the LAAS building at Stanford and each antenna element was connected to the front end box via 4 equal-length low-loss cables. The signal is mixed down to 47.75 MHz and passes through a number of filters, LNA's, and an AGC, after which the signal is sent to the data sampling PC. The data sampling PC uses two 2-channel ADC cards, and the signal is band-pass sampled at 11.25 MHz, resulting in 2.74 MHz IF signal that's stored on the hard drive [2].

The data was collected in parallel with a Novatel OEM 4 receiver which provided the PRN number, elevation, and azimuth angles of the satellites in view.

Beam-Forming Algorithm

The fundamental idea of any phased antenna array system is to phase align all the received signals in a particular spatial direction, and combining them to obtain a more powerful signal. By adjusting the inter-element phase shifts, one can control the direction from which the desired signal being received by the antenna elements of the array combine in-phase [3,4].

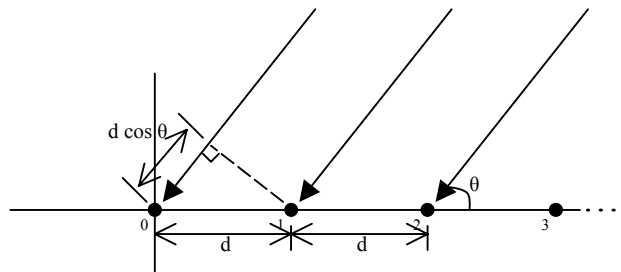


Figure 4. 2D Linear Array Example

Figure 4 illustrates a 2D example of a linear array with incident incoming signal angle, θ . Assuming isotropic receiving antenna elements, the received power, or the Array Factor, of the above array can be represented as follows.

$$\begin{aligned}
 AF &= W_0 A_0 + W_1 A_0 e^{j2\pi f d \cos \theta} + W_2 A_0 e^{j2\pi f 2d \cos \theta} + \dots \\
 &= \sum_{n=0}^{N-1} W_n A_0 e^{j2\pi f n d \cos \theta}
 \end{aligned} \quad (1)$$

where W_n is the gain applied to antenna element n . If the applied gain is defined as follows,

$$W_n = e^{jn\alpha} \quad (2)$$

α being the inter-element phase shift that is being driven to scan the beam. Thus we get,

$$AF = \sum_{n=0}^{N-1} A_0 e^{jn(2\pi fd \cos \theta + \alpha)} \quad (3)$$

α can be chosen so that the incident signal from direction θ at each antenna element will be perfectly in phase, thus resulting in a received signal whose amplitude (or power) will be N times that from a single antenna element.

$$\alpha = -2\pi fd \cos \theta \quad (4)$$

$$AF = \sum_{n=0}^{N-1} A_0 = NA_0 \quad (5)$$

However, if the scanning phase α were slightly off, each element's signal will be slightly out of phase, and the resulting power of the output will be less than optimal. One can clearly see that this will also lead to some phase error in the composite array output, and as mentioned before, any unwanted effect on the phase is undesirable for JPALS, due to the extremely stringent integrity and accuracy requirements on the carrier phase differential system.

$$\alpha = -2\pi fd \cos \theta + \Delta\alpha \quad (6)$$

$$AF = \sum_{n=0}^{N-1} A_0 e^{jn(\Delta\alpha)} \quad (7)$$

In 3D, the required phase shifts to form the beam rearranges as follows.

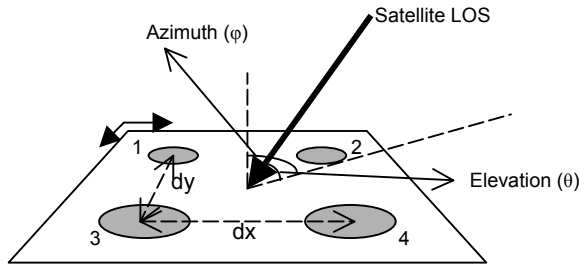


Figure 5. 2x2 Rectangular Array 3D

$$\alpha_{x-dir} = 2\pi fd_x \cos(\theta) \sin(\phi) \quad (8)$$

$$\alpha_{y-dir} = 2\pi fd_y \cos(\theta) \cos(\phi) \quad (9)$$

$$\alpha_{xy-dir} = \alpha_{x-dir} + \alpha_{y-dir} \quad (10)$$

It should be made clear that for this paper, there is no implementation of a beam-steering algorithm. The real data, collected using the hardware data collection system, is of a short enough duration that the line-of-sight vectors to each satellite in view are stationary. Thus, there will not be any steering of the beam. Rather all possible

beams, with some finite resolution, are constructed and compared.

Phase Shifting Implementation

The required phase shift in each channel to form a beam in any desired direction was given in the previous section. To achieve the required phase shift, the signal going into each channel will be split into its in-phase and quadrature components, each weighted accordingly, and recombined. Figure 6 shown below illustrates this process.

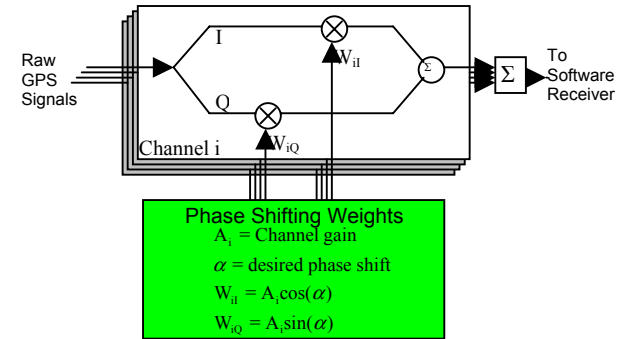


Figure 6. Phase Shift Implementation

Software Receiver

In order to study the effects of beam-forming, a software receiver was implemented. The receiver functionality diagram of the receiver that was implemented is shown below [5].

By implementing the receiver in software, parameters of interest to the analysis were much more easily accessible. The beam-forming algorithm's effect on the correlation peak power (max/mean of the correlation function) and the carrier output of the phase lock loop (PLL) will be investigated.

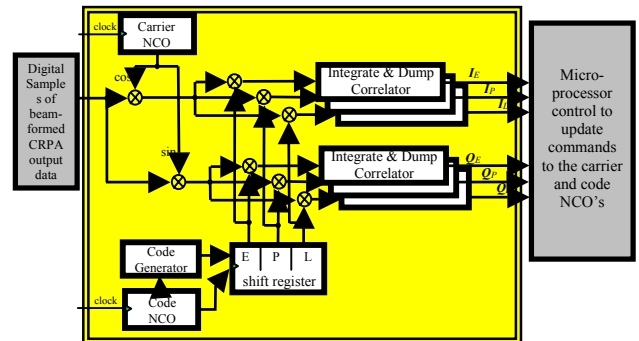


Figure 6. Software Receiver Functionality

RESULTS

Phase Error Map

As mentioned previously, applying a CRPA array for JPALS use may lead to errors in the beam-pointing direction. This could result from any uncertainties in the knowledge of the antenna arrays orientation. If there are pointing errors, the phase-shifted signals in the 4 channels would not combine in-phase. This will lead to some resultant error in the phase of the array output signal with respect to what the phase should be. Such effects, if unaccounted for, will reduce the accuracy/error budget and have unwanted adverse effects on the integrity budget.

The following plot quantifies this effect on the phase of the carrier signal output of the PLL after the PLL has achieved lock. An intentional pointing error has been injected into the beam-forming algorithm, and the resultant difference in phase between the phase-locked beam-formed signal and the phase-locked “truth” signal is plotted. By using simulated signals, it is possible to generate a “truth” signal that is representative of the signal that should be received at the origin of the array coordinate system. The phase error map (Figure 7 below in units of degrees) is plotted as a function of the elevation and azimuth of the beam that is formed. Figure 8 shows the corresponding correlation peak power pattern (units in dBs) as a function of the elevation and azimuth of the beam.

Phase Error Pattern

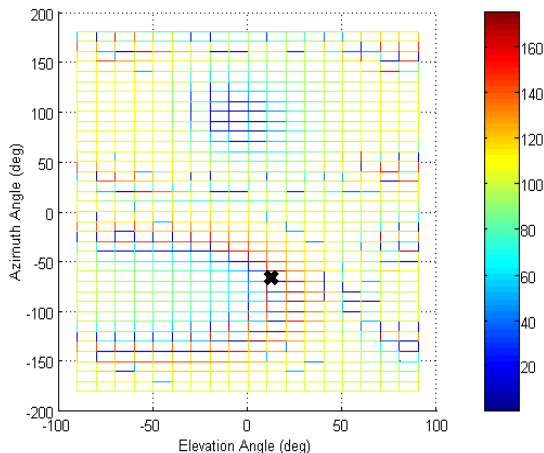


Figure 7. Phase Error Map for 2x2 Array

The ‘x’ on Figure 7 and Figure 8 indicate the incoming direction of the signal. When the beam is pointed towards that direction, the resultant phase error is close to zero, i.e. the 4 channels combine in-phase. It is also shown on Figure 8 that this is the direction that gives maximum

gain, thus resulting in the highest correlation peak power. It is interesting to note that along a certain direction, even if there is a pointing error, the 4 channels combine in such a way that the resulting error on the phase is very small. It does, however, result in lower received power as can be seen in the corresponding correlation peak power pattern shown in Figure 8. This is representative of 2 of the channels combining out-of-phase and canceling each other out, rather than combining in-phase to form a more powerful resultant signal. The result is a lower received power even though impact on phase was minimized. Another point of interest is that in certain other directions, the error in phase grows drastically.

Correlation Peak Power Pattern

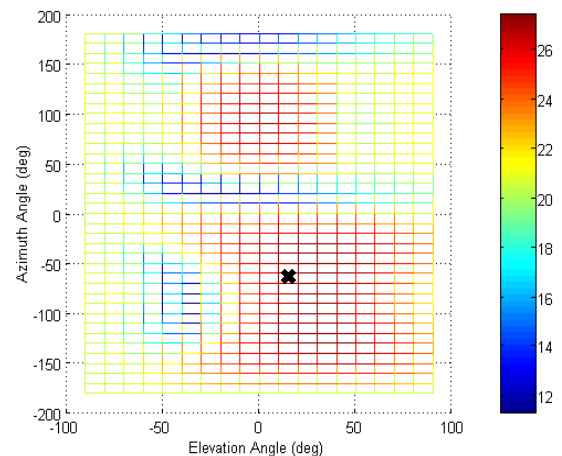


Figure 8. Correlation Peak Power Pattern

Interference Rejection

The software signal generator package allowed for the injection of interference signals into the signal data set and the beam-forming algorithm’s ability to reject interference signals was investigated for the 2x2 rectangular array configuration. Two different types of interference signals were studied: CW and pulsed.

Figure 9 shows the results from the CW interference signal injection at L1. The x axis shows the degree offset between the desired incident signal and the interference source in azimuth. The y axis shows the correlation peak power obtained for that PRN.

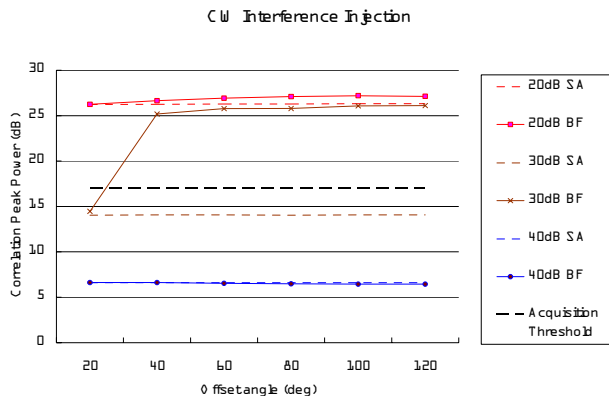


Figure 9. CW Interference Rejection Performance

The solid colored lines represent the correlation peak powers for the beam-formed signal (marked BF on legend), while the dashed colored lines represent the correlation peak power observed for a stand alone single antenna (marked SA on legend) subject to each corresponding interference signal. The thick black dashed line represents the threshold above which the signal is acquired. In the case of the 20 dB CW interference, the interference signal is of low enough power that it does not impact the stand alone case significantly, and thus, there is not much gain obtained by beam-forming the signal. On the other hand, when the interference signal power is increased to 40 dB J/S, it is too powerful and overwhelms the correlation function, even for this four antenna beam-formed signal, and the signal acquisition fails. In between, for the 30 dB J/S interference signal, when the interference source is 20° offset from the incident signal direction, the interference is too close in proximity to the desired signal and it is unacquirable, even with beam-forming. However, as that offset becomes larger (greater than 40°), beam-forming gives us enough leverage to be able to acquire that signal.

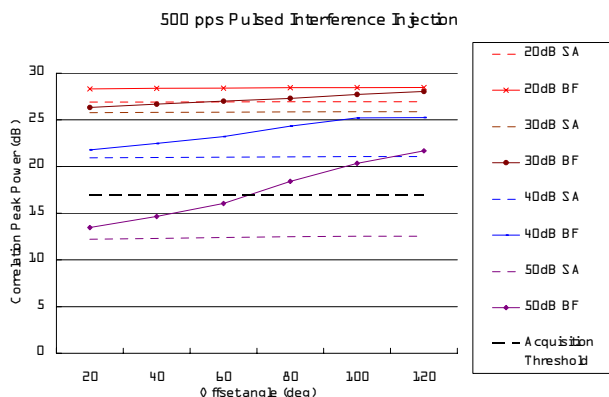


Figure 10. 500 pps Pulsed Interference Rejection Performance

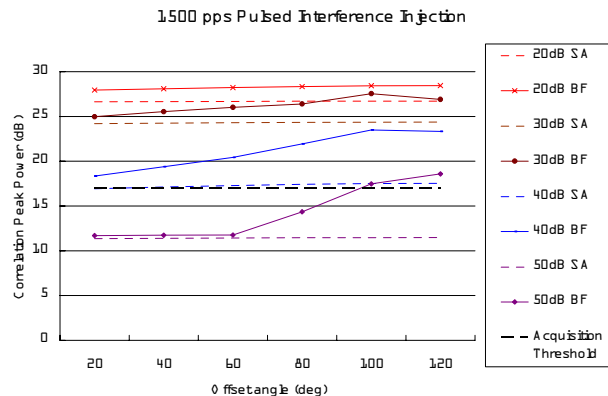


Figure 11. 1500 pps Pulsed Interference Rejection Performance

Figures 10 and 11 show results for similar analysis done for a pulsed interference signal with 500 and 1500 pulses per second (pps) respectively.

For both cases, the amount of benefit afforded by beam-forming increases as the interference signal power (J/S) is increased. For 500 pps, beam-forming allows the acquisition of a signal that is subject to 50 dB J/S power as long as it is offset greater than 80° from the signal direction. For 1500 pps, the 40 dB J/S interference signal causes the correlation power to be just on the threshold of acquisition for the stand alone case. Naturally, the signal can be definitively acquired by beam-forming. The 50 dB J/S 1500 pps pulsed interference signal nearly overwhelms even the beam-former, but acquisition is achieved at greater than 100° offset.

Hardware Validation

Real GPS data was taken to validate the beam-forming algorithm implementation and the software signal simulator. We will investigate two different antenna array configurations: a 2 element linear array, and a 2x2 rectangular array. In each case, a simulated data set was constructed to emulate the actual data collected using information provided by the Novatel OEM 4 receiver that was running in parallel to the data collection system.

Figure 12 shows the 3D correlation peak power pattern of the beam-formed signal for the 2 element linear array using simulated data. Figure 13 shows the corresponding pattern using real GPS data obtained using the hardware data acquisition system. We are looking for a match between the two to validate the simulation with real data.

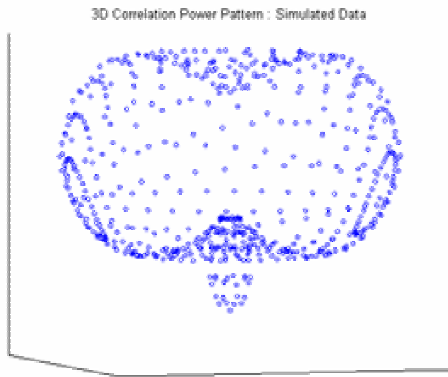


Figure 12. 3D Correlation Peak Power Pattern for 2 Element Linear Array using Simulated Data

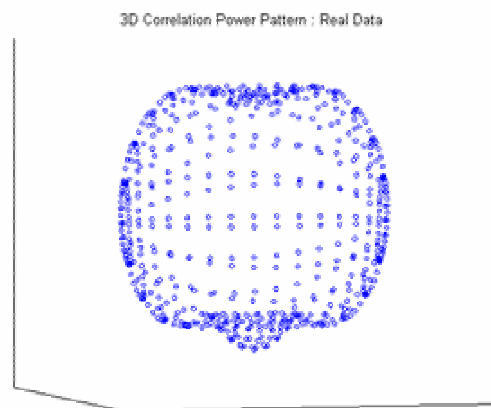


Figure 13. 3D Correlation Peak Power Pattern for 2 Element Linear Array using Real GPS Data

The two patterns (Figures 12 and 13) show good correspondence. However, they also do show some subtle differences. Mainly, the pattern using simulated data has features that are sharper. This can be attributed to the fact that the simulation assumes perfect isotropic receiving elements with low noise, while the real data includes all the noise elements injected by the antenna, and the front-end box. The amount of noise in the data set was a difficult parameter to estimate and emulate exactly in the simulated data set. Another source of error could be the mutual coupling effects in the real GPS data that are not taken into account in the simulated data. Finally, the error in the orientation of the array during data collection may be another source of the difference. As mentioned previously, the knowledge of the array orientation is crucial to accurately pointing the beam. In this case, the antenna array was oriented towards the magnetic north and assumed to be flat parallel to the surface of the earth. Any small errors that may exist in those assumptions regarding the orientation of the array will lead to subtle differences in the pattern between the simulated and the actual case.

Similar analysis was done for a 2x2 rectangular array configuration, and is presented below. It should be pointed out that the 3D patterns for this configuration were rather difficult to distinguish visually. Thus the results are presented as mesh plots as a function of the elevation and azimuth angles of the beam-pointing direction for greater ease in comparison.

Figure 14 shows the correlation peak power pattern for a 2x2 antenna array using simulated data. Figure 15 shows the corresponding pattern using real GPS data collected through the hardware data collection system. In comparing the two patterns, they are remarkably similar. Subtle differences may be attributed to the explanations given above, but the two patterns seem to show a better match than shown for the 2 element linear array case. This can be attributed to the fact that this data set was taken using antennas and cables that were superior in terms of noise performance. It is also possible that the effects of mutual coupling were smaller as a result of the different antennas and cables.

From the results of both the 2 element linear array, and the 2x2 rectangular array analyses, we can safely say that the software simulator and the beam-forming algorithm implementation are validated.

Correlation Peak Power Pattern from Simulated Data

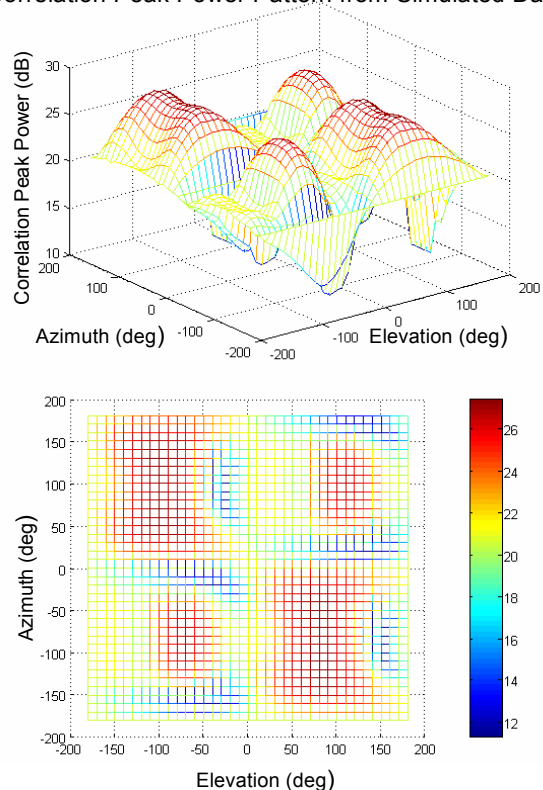


Figure 14. Correlation Peak Power Pattern for 2x2 Array using Simulated Data

Correlation Peak Power Pattern from Actual GPS Data

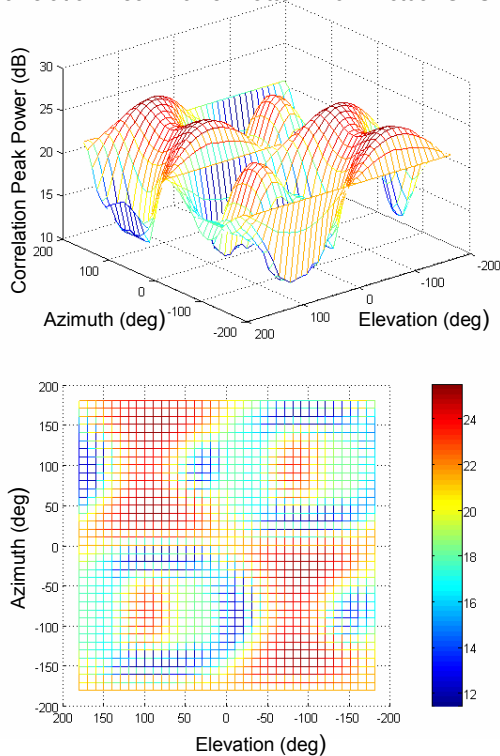


Figure 15. Correlation Peak Power Pattern for 2x2 Array using real GPS Data

Sampling Bit Requirement for Beam-forming

Finally, we investigated if there was a requirement for the number of sampling bits to successfully point a beam. This could be a point of consideration for the hardware requirements for implementing a CRPA design for JPALS use. The simulated data set for the 2 element linear array, discussed above, was converted to a 1 bit data set, and the 3D correlation peak power pattern was formed and is presented below in figure 16.

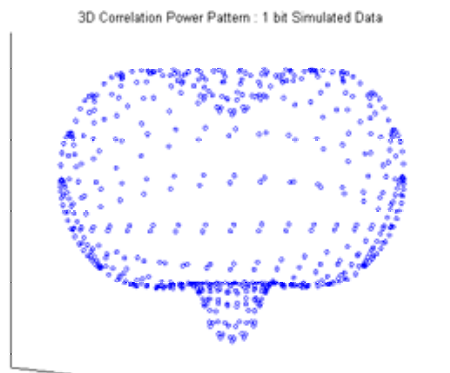


Figure 16. 3D Correlation Peak Power Pattern for 2 Element Linear Array using 1 bit Sampled Data

Comparing Figure 16 to Figure 12 shows similar looking patterns. Figure 12 is the 3D correlation peak power pattern using 16 bit sampled data. The figure 16 above shows that even with 1 bit sampled data, it is possible to form a beam, although it does lose some sharp features near the “backlobe” where the nulls would be formed. This is due to the lack of phase resolution afforded by 1 bit data, and therefore is unsuitable for use in the JPALS environment, where accurate sharp beams/nulls are desirable. A possible design consideration presents itself in the trade-off between the phase resolution afforded by higher bit samples and the cost of the hardware to implement.

CONCLUSIONS

A software tool was developed and validated that allows an in-depth investigation of the effects of a beam-forming algorithm on a GPS signal. This tool was used to study the phase bias that’s introduced into the signal as a function of beam-pointing error. The results show that the phase error shows highly spatial dependencies. The errors are much more sensitive along some directions than others.

The beam-forming algorithm’s ability to reject CW and pulsed interference signals in the acquisition of signals was also presented. Finally, it was shown that 1 bit data samples are sufficient to perform and reap the benefits of beam-forming. However, 1 bit data does not provide enough phase resolution to be of functional use in the JPALS environment.

Having validated the software signal generator and the beam-forming algorithm implementation, this tool can be used to simulate arrays of larger size (more elements) that are more representative of actual CRPAs that may actually be implemented for JPALS, and to investigate beam/null steering algorithms. This can be done since the mechanism by which beam/null steering algorithms steer the beam is the phase shifting methods presented in this paper.

ACKNOWLEDGMENTS

The authors would like to acknowledge and thank the Naval Air Warfare Center Aircraft Division (NAWCAD) who funded this research.

REFERENCES

- [1] “System Requirement Document for SRGPS” R2 Baseline ver. 1.0, August 2003
- [2] Gromov, Konstantin G., “GIDL: Generalized Interference Detection and Localization System”, Ph.D. Thesis, Stanford University, 2002

[3] Stutzman, Warren L., and Thiele, Gary A., "Antenna Theory and Design" 2nd edition, John Wiley & Sons Inc., 1998

[4] Balanis, Constantine A., "Antenna Theory: Analysis and Design" 2nd edition, John Wiley & Sons Inc., 1997

[5] Forssell, Börje, "Radionavigation Systems", Prentice Hall, 1991